

Development of Electro Active Polymers Configurations to Monitor and Control Deployable Space Structures

S. Baldacci¹; L. Serafini¹; V. S. Zolesi¹; F. Thurecht²; E. K. Pfeiffer²; P. Sommer Larsen³; F. Carpi⁴; D. De Rossi⁴; L. Lampani*; P. Gaudenzi*;

¹Kayser Italia Srl, IT; ²High Performance Space Structure Systems GmbH, DE; ³RISOE National Laboratory - Technical University of Denmark, DK; ⁴Centro Piaggio - Pisa University, IT; *DIAA - University of Rome La Sapienza, IT

In the framework of the ESA funded project EAP (Electro Active Polymers) an international team of universities and companies led by Kayser Italia Srl has studied and developed applications of EAP to investigate the possibility to monitor and control inflatable and deployable lightweight space structures. Different configurations of EAP have been studied and developed aiming at damping the vibrations of a long inflated-rigidized boom and at the shaping of reflector like structures. Novel configurations of electro-active polymers have been designed and manufactured with the aim of testing their capabilities on breadboards which are representative of space structures. The work on the development and characterization of the EAP configurations is presented first along with experimental data and simulations run with models purposely developed. Secondly the breadboards used to test the capabilities of the configurations are presented and explained. A section is dedicated to the modelling and simulation of the configurations and the breadboards because it represents a rather important part of this project. Lastly the experimental results of the performance test are presented and discussed.

1. EAP CONFIGURATIONS

We term „configurations“ the actuators manufactured with EAP. Two important key features of these configurations are the softness/fold-ability/lightweight and the integration at device level of actuation and sensing capabilities. Another strong point is the possibility to embed them into foldable structures on ground and then deploy them once in space.

1.1. Multilayer Dielectric Elastomer Actuators (DEA) with Smart Compliant Electrodes (SCE)

DEA-SCE is an electrostatic actuator technology [1]. It comprises a 20-60 micron thick elastomer film sandwiched between two compliant electrodes. It is a flexible capacitor. When the electrodes are charged at high voltages (typical range of Kilovolts), the two electrodes attract each other and compress the film. The compliant electrodes allows for a corresponding extension in the film plane whereas volume of the elastomer remains constant during operation.

The smart compliant electrodes consist of a microscopic wave pattern imprinted in the film [2]. The film surfaces are metallised, which makes the film compliant in the direction of the wave pattern and rigid in the orthogonal direction. The actuator is unidirectional. FIG. 1 illustrates the principle [3] [4].

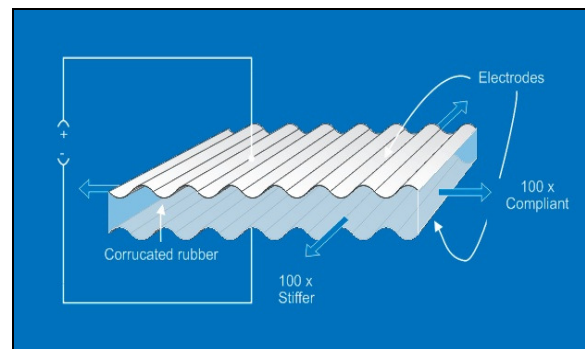


FIG. 1 Corrugated compliant electrodes

The actuators come as sheets of very soft rubber with metal-coated electrodes. These sheets may be rolled to a band. Application of up to 2.5 kV will extend the actuator up to 10%.

In order to do work, the actuator must be stretched or pre-loaded. Upon charging the actuator, it extends. Another actuator (working as antagonist) may stretch the actuator further. Alternatively, the embedding structure may do the job. Upon discharging, the actuator returns to its original position, due to its elasticity. Work is done against the load.

Extension as function of applied voltage is governed by the balance between the electrical induced stress, the load on the actuator and the relation between stress and strain:

$$\sigma_E + \sigma_m = G \left(\lambda^2 - \frac{1}{\lambda^2} \right) \quad \text{Equation (1)}$$

$$\sigma_E = \epsilon E^2$$

Where E is the electrical field, σ_m the true stress corresponding to the constant applied load and σ_E the

Maxwell stress.

λ is the strain ratio between the instant length and original length and G is the shear modulus.

The sensing property is inherent to this configuration since it is a flexible capacitor. When a compliant electrode is extended it becomes thinner and it shows an electric capacitance change. The pictures below shows a prototype of the developed configuration with a central part of multilayer actuator and two side strips dedicated to sensing including the corresponding copper electrodes.

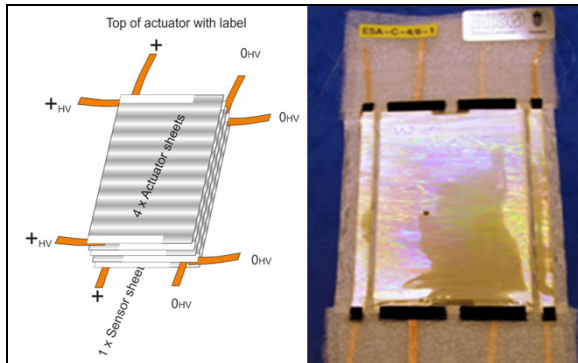


FIG. 2 Prototype of multilayer elastomer actuator/sensor

The table below reports typical dimensions and performance of a 4 sheet multilayer actuator including the characteristics of the material. The bare sheets where produced by Danfoss A/S in Denmark".

Size [mm]	Max Extension [%]	Load [g]	Speed [Hz]	Max Voltage [Volt]
100X75X0.15	10	200	5	2500
Material	Young modulus [MPa]	ϵ_r [C ² /(m ² N)]		
Silicone Wacker Elastosil RT 625	1	2.8		

TAB. 1 Main features of a multilayer elastomer actuator

DEA-SCE have been electromechanically characterized. Two main characterization test results are reported in this work. The actuation performances is represented by an extension versus applied potential curve in FIG. 3 (at isotonic condition of optimal load of 200 grams).

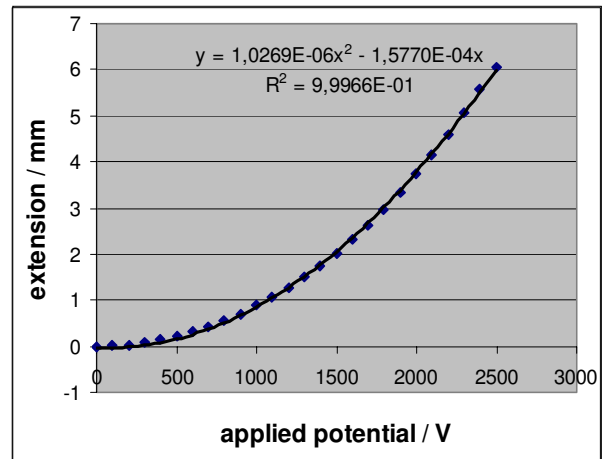


FIG. 3 Actuation characteristic of multilayer DEA-SCE with numerical curve fitting

The capacity of the sensor part depends linearly on the extension. The general rule is that the capacity changes 2% per mm extension independent of the cause of extension: passive load or applied potential. The sensing performances are given in the extension versus capacitance curve below.

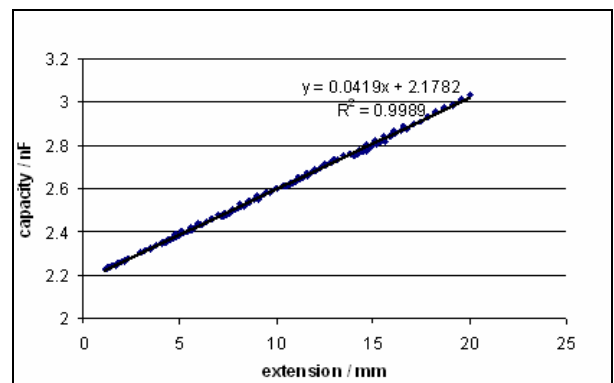


FIG. 4 Sensing characteristic of multilayer DEA-SCE with numerical curve fitting

The transient response of the actuator/sensor after applying a step potential is essential for its use in a controlled system. The actuator will typically work against a tension applied by a spring while moving a mass. The step response analysis shows that the response occurred within 30-60 ms. 30 ms is the sampling time and hence the minimum response time measurable. The plots of FIG. 5 reports the response of the actuator load to a 2.5 kV voltage step and the corresponding response of the capacitive sensor part.

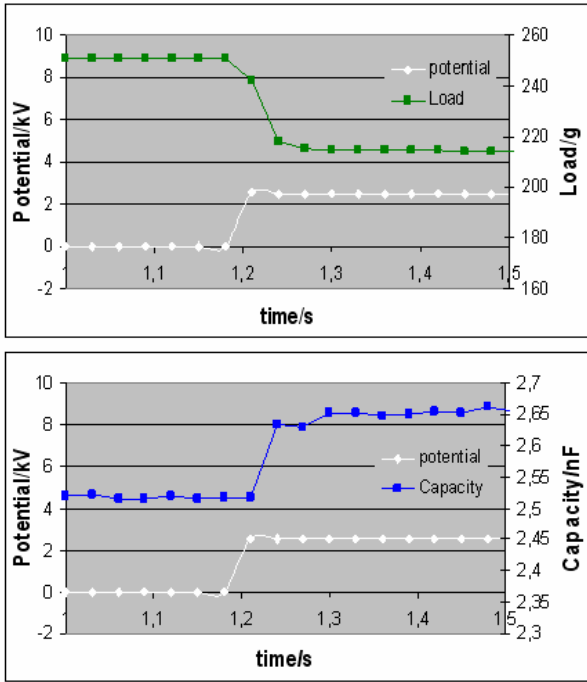


FIG. 5 2.5 KV step response of actuator and sensor part

The actuators work against a spring and the total moving mass consist partly of the springs mass, partly of the actuator mass and the passive material moving with the actuator.

1.2. Dielectric elastomer Bubble Actuator with piezo-capacitive displacement sensor

[5] [6] This type of device is composed by two parts. the actuator part consists of a thin elastomeric circular membrane (with a diameter of 30 mm and a thickness of about 0.8 mm), whose opposite surfaces are coupled to two compliant concentric circular electrodes, as presented in the sketch of FIG. 6. The sensing part consists of a compliant electrode coupled to the lower face of the actuator and insulated from it by means of a second elastomeric disc in order to implement a piezo-capacitive sensing. A second sensing electrode is used: and it consists of an insulated metallised hemisphere, which serves also as a support for the whole structure.

The rigid hemispheric substrate is coupled to a planar supporting surface. The top of the hemisphere stands approximately 3 mm above the support surface. A concentric ring-like frame provides boundary constraints for the actuator.

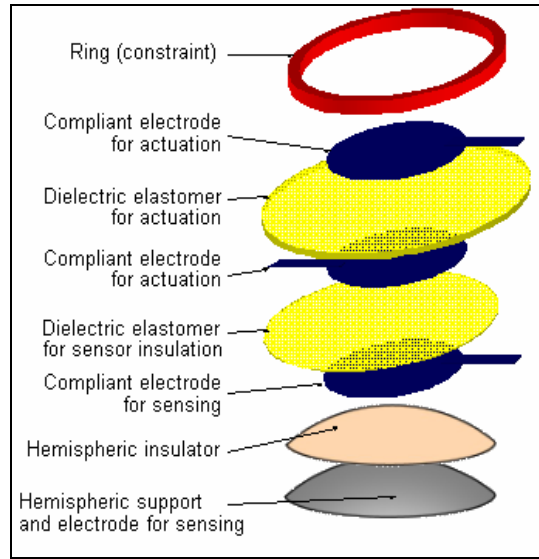


FIG. 6 Exploded view of an EAP bubble actuator with integrated sensing.

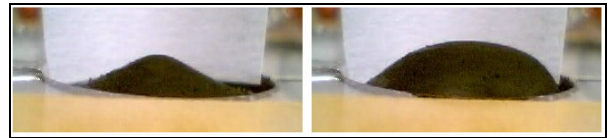


FIG. 7 Prototype bubble actuator/sensor: (left) device at rest; (right) device under electrical activation.

The resulting final shape of the constrained membrane is sketched below.

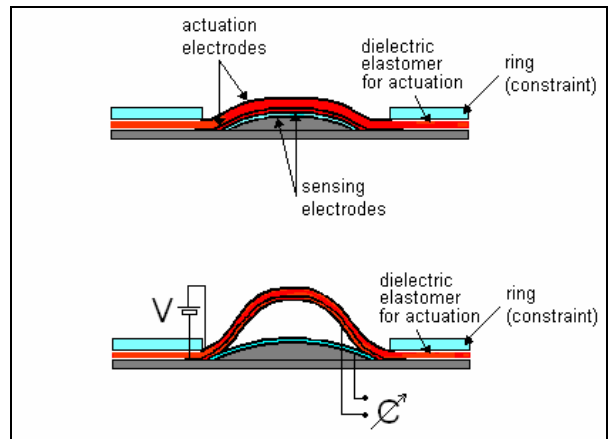


FIG. 8 Schematic view (section) of a bubble actuator and sensor.

When a high voltage is applied between the actuation electrodes, the opposite charges on them generate an attractive force, which compresses at constant volume the intermediate dielectric membrane. Accordingly, its thickness is reduced while its area is increased. Because of the boundary ring, the membrane cannot expand in radial direction. Moreover, the initial out-of-plane geometry determined by the underlying hemisphere makes the membrane lift up; therefore, the

actuation consists of an out-of-plane displacement of the membrane (see FIG. 8).

At the same time, the actuation can be monitored by reading the variation of the sensing capacitance (see FIG. 8).

Conversely, without any initial pre-deformation the actuation would generate an uncontrolled wrinkling of the surface. This simple layout allows a passive way of providing the appropriate boundary conditions for active buckling, without additional components and instrumentation (e.g. an underlying pressurised/depressurised chamber).

Prototypes of this kind of actuator/sensor were fabricated with a silicone rubber (TC-5005 A/B-C, BJB Enterprises Inc., U.S.A.), having an elastic modulus of approximately 50 KPa. The material was shaped as a circular membrane. The support was made of a dielectric resin. The electrodes were made of a thin layer of a conductive silicone/graphite mixture, applied on the upper and lower surfaces of the circular elastomeric membranes. Both electrodes have a circular shape and are concentric with the membrane.

Prototype devices were electromechanically characterized in terms of actuation and sensing capabilities. FIG. 9 reports displacement and capacitive sensing performances in the actuation range 0-8.5 kV.

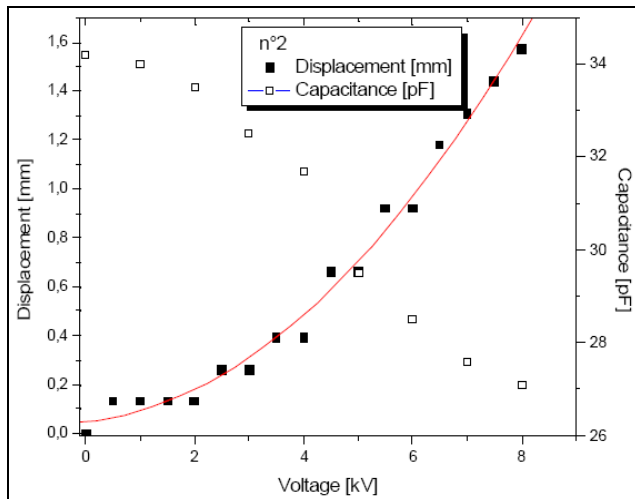


FIG. 9 Actuation and sensing performances (device with no external load).

2. DEMONSTRATIVE BREADBOARDS

2.1. Electronic control system

The main piece of hardware of the electronic control system is the Control Unit board. It is based on a Xilinx FPGA Spartan with 400 KGates. The main functionalities are:

- Interface of 35 EAP sensors to measure their capacity (The capacity measurement is carried out

by measuring the charge time of an oscillator where the capacity is inserted in a circuit with a reference resistor)

- Acquire acceleration signals from two tri-axial digital accelerometers fitted in the mechanical structure
- Drive 30 analogue outputs for High Voltage modules to drive EAP actuators
- Perform closed-loop controls of vibration damping
- Communicate with a PC via serial link RS232 at 115200 bps.
- Monitor the signals acquired from the breadboards

The FPGA processes the acquired data for closed-loop controls and signal monitoring. It reads commands from a PC connected through a serial line, it executes them and it prepares the output answers to be sent back. The FPGA core is a state machine that manages all the analogue and digital sub-modules of the Control Unit.

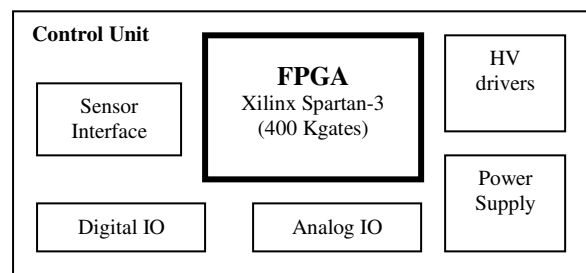


FIG. 10 Block diagram of the electronic Control Unit

2.2. Inflatable rigidized carbon fiber boom

This breadboard was used to study the possibility of damping the vibrations of a boom with a controlling algorithm. A 3.5 meter boom has been manufactured by using pre-impregnated carbon fiber foils rolled over an inflated nylon support. After laying down of the fibers the boom has been cured at high temperature and the nylon tube deflated and removed.

The boom is fitted with four DEA-SCE stations placed along its cross section. An additional mass in the free end was added to scale vibration frequencies down. The boom is fixed on the ground to a heavy steel plate with four accelerometers placed as shown FIG. 11.

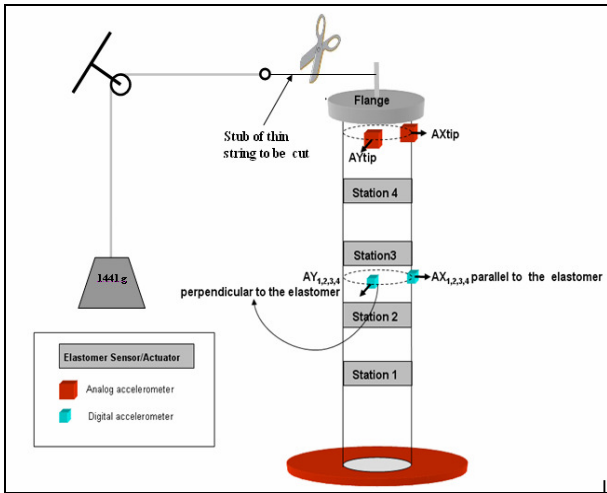


FIG. 11 Boom equipped with EAP stations and setup for testing

The DEA-SCE configurations were fitted in the cross section of the boom at manufacturing time so that the boom section becomes slightly oval and the actuators have the right amount of pretension force to work at optimum conditions.

In a preliminary study a damping mechanism using an actively controlled deformation of the cross section of the boom was identified, which fitted to the capabilities of the actuators. The DEA-SCE will be pre-stressed to the correct value and after curing the pressure will be released. The elastic forces of the cross section of the boom counteract the elastic forces of the DEA-SCE. When a voltage is applied to the DEA-SCE it will stretch and the cross section is altered to a more circular shape. The differences in bending stiffness of a circular to elliptical boom can be used to actively dampen boom oscillations.

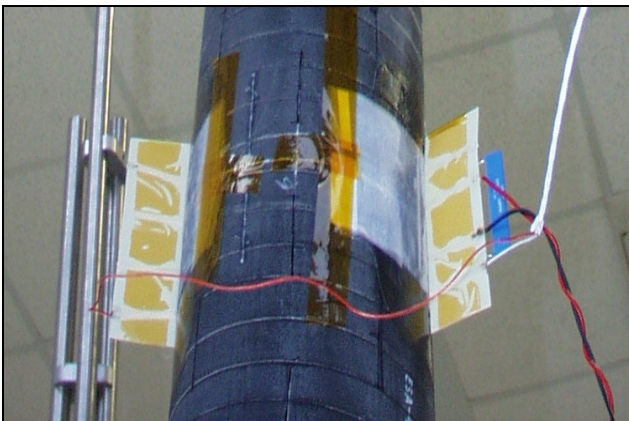


FIG. 12 Boom with DEA-SCE embedded in its cross section

All the stations are equipped with high voltage actuation electronics and sensor reading modules implemented by Time to Digital Conversion circuitry (TDC) placed by the boom and attached to a surrounding scaffolding. The whole system was controlled by an electronic unit which in turn was connected to a PC for monitoring and control. The breadboard is operated by imposing a certain bending to its free top end and then releasing it in order to induce reproducible vibrations in to the structure.



FIG. 13 View inside boom with DEA-SCE embedded

2.3. Matrix of Bubble Actuators

Bubble actuators are ideally suited to actuate matrix like systems.



FIG. 14 Bubble matrix breadboard, partly equipped with actuators

A 4X4 matrix made of 3 cm bubble actuators supporting a thin foil of silicone has been manufactured to investigate the possibility to achieve a surface shape control with EAP configurations. Each bubble in the matrix has integrated sensing capability and therefore opens up the possibility to control a surface shape with some degree of resolution.

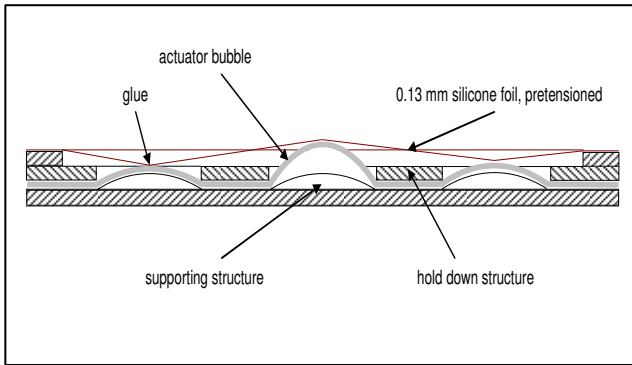


FIG. 15 Cross section of bubble matrix with silicone foil on top

3. NUMERICAL MODELLING

3.1. Inflatable rigidized carbon fiber boom

[7] A Finite Element Method (FEM) analysis model of the DEA-SCE configuration has been developed and tested against experimental results in order to characterize the configurations in different loading and actuation conditions.

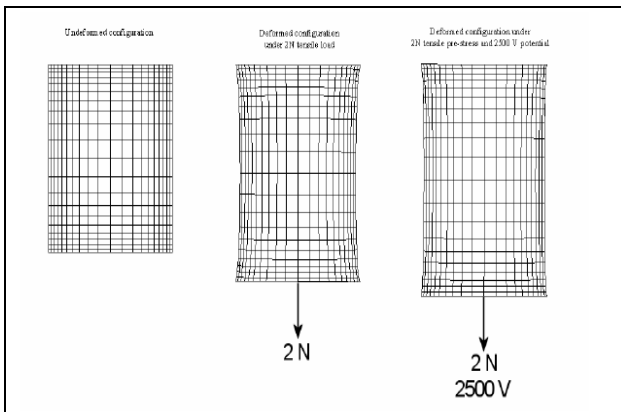


FIG. 16 FEM model of the configuration tested at different loading and actuation conditions

The following graphs shows the comparison between the model simulations and the experimental results for different conditions. The first graph represents the load versus extension relationship and the second the extension versus applied voltage for a given preload (optimum preload = 2 N).

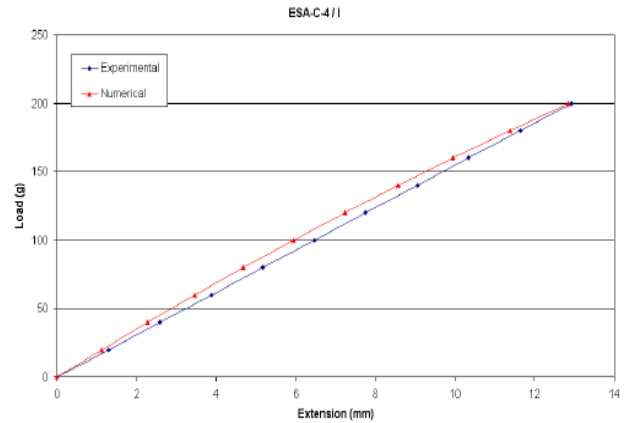


FIG. 17 Passive elastic characteristic of the configuration (0 Volts)

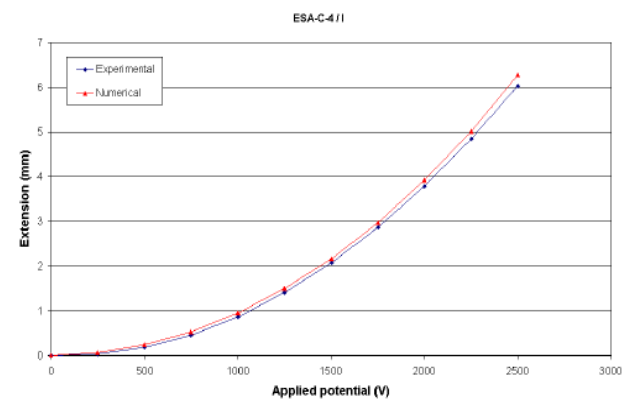


FIG. 18 Active characteristic of the configuration at optimum load (2 N)

The inflatable rigidized boom used as a breadboard was modelled through FEM analysis and then the model of the boom was integrated with the models of the DEA-SCE configurations as depicted in FIG. 19.

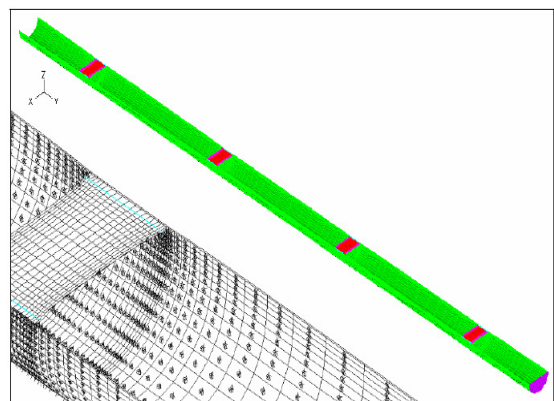


FIG. 19 FEM model of the boom with four integrated configurations

The numerical model of the integrated boom has required a phase of calibration to achieve a good correlation between numerical simulations and experimental data taken during laboratory characterization tests.

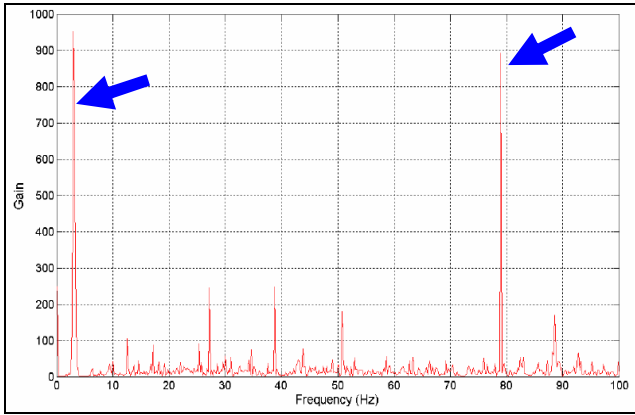


FIG. 20 Spectral analysis of the boom vibrations (first bending mode)

Measurements have shown that the first and the second bending frequency respectively correspond to 2.75 Hz and 78 Hz. By adjusting the Young and Shear modulus of the carbon fibre used in the production of the boom and by adjusting also its density a good fitting of numerical models and experimental data was achieved.

In order to develop a control algorithm to reduce the amplitude of the oscillation of the boom, induced by an external perturbation, a multi-body model was created. The model simulates the experimental set up shown above in FIG. 11. In the tested configuration the stations#1, #3 and #4 worked only as actuators, whereas station#2 worked only as sensor. This choice was due to technical reasons and to the fact that best sensing capability for the first bending mode is achieved by the sensor of station #2. The boom structure is represented as a flexible body. The NASTRAN model is imported in DCAP software package (*Dynamics and Control Analysis Package*) through the *pre_flex* routine. Each DEA-SCE actuator is modelled with a couple of actuators0. In the DCAP model the actuators play a double role: they work to apply a preload (all stations #) and to apply the controlling action (stations #1,#3,#4).

An accelerometer is fitted on the free end of the boom to observe the actual oscillations of the structure and to assess the effectiveness of the control, but it is not used inside the control loop. The only information used in the control algorithm comes from the sensor in station #2.

3.2. Bubble Actuators

In order to model this kind of actuator, as first step we need to take in account that the elastomers moves out of a planet. In this way the mathematical formulation of the elastomers implemented into the ADINA© code has to be modified to improve this capability.

The Maxwell stress state of the elastomer has to be evaluated in each point taking into account that the local reference system, placed locally along the surface of the bubble (electrodes), has to follow the deformation of the surface itself. The Maxwell stress matrix is calculated through a rotation matrix, rotation from the global reference system, laying in a plane, to the local one. The hypothesis that the electric field is normal to the electrodes and that the polarization vector is aligned to the electric field is assumed.

A numerical three-dimensional model has been developed for the bubble actuator. Simulations with the numerical models have shown a good degree of correlation with the experimental results even though the structural behaviour of such a configuration is rather complex and it is difficult to achieve perfect fitting of the model with the measurements(see FIG. 21).

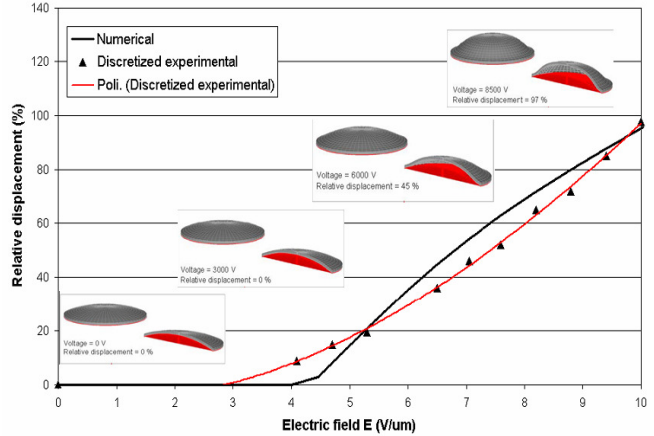


FIG. 21 Simulated and experimental characteristics of the bubble actuator

In order to simulate the static and dynamic behaviour of the bubble in a closed loop position control, a simplified one-dimensional model of spring-mass-damper kind has been developed.

For the mass estimation of 0.5 g is taken. To estimate the stiffness, a frequency/modal analysis on the three-dimensional finite element model is performed. The first natural frequency of the bubble is about 15 Hz.

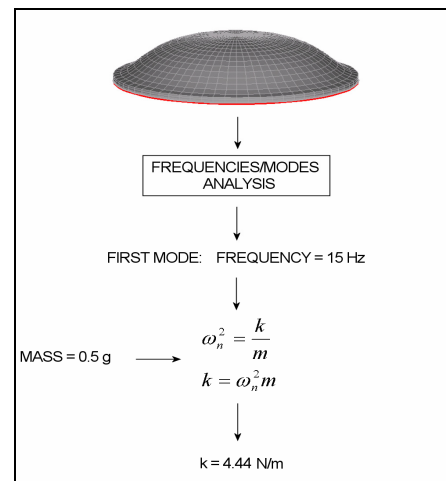


FIG. 22 Simplified dynamic modelling of the bubble actuator

Moreover the [high-voltage-drive] versus [elongation] versus [capacitive-sensing] characteristic of the bubble has been obtained at different loading conditions (0.7 grams, 1.4 grams, 2.1 grams). This static characterization has been integrated with the simplified dynamic model to obtain a complete static-dynamic model to run simulations with.

The model has been tested in a closed loop PI control.

The input signal was a ramp of driving voltage and the system was disturbed with a load added to the mass of the bubble.

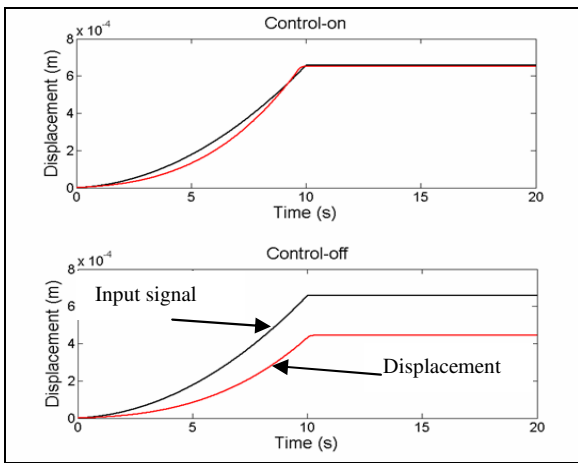


FIG. 23 Response of the controlled bubble actuator

The picture above shows the simulated response of the system with and without a control when the bubble actuator is disturbed with a loading mass.

4. TESTS

4.1. Carbon fibre boom

Laboratory tests were carried out to assess the vibration damping capabilities of a system composed by the inflatable rigidized boom connected in a closed loop control.

The control was composed of an electronic unit, sensor reading electronics and high voltage drivers for the actuators. The system is described in the picture below

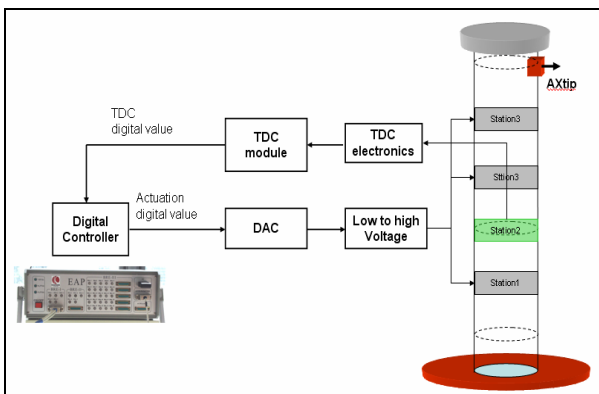


FIG. 24 Integration of the boom with the controlling system

The final objectives of these tests were to assess the capability of the EAP configurations used to monitor and control large structures and to assess possible vibration damping algorithms to be implemented in the electronic hardware. Several session of tests and simulation were carried out in parallel to achieve a fitting between experimental data and numerical simulation and also to identify, through simulation first, the best performing algorithm to dampen the vibrations

of the boom.

The tests were carried out by comparing the boom vibrations in the case of free damping and controlled damping. Vibration of the boom was induced by cutting the string that held the boom bent as shown in FIG. 11. Data were acquired both from the station#2 sensing and from the tip accelerometer. The results were averaged over a total of 10 acquisitions each for the free and the controlled boom cases.

The following table summarizes the test results :

Station#2 Sensing			
Free damping		Controlled damping	
Exponential decay time constant (stdev=2.05%)	First mode frequency (stdev=0.46%)	Exponential decay time constant (stdev=3.35%)	First mode frequency (stdev=0.49%)
7.68 [sec.]	2.77 [Hz]	5.61 [sec.]	2.77 [Hz]
Tip Accelerometer			
Free damping		Controlled damping	
Exponential decay time constant (stdev=1.85%)	First mode frequency (stdev=0%)	Exponential decay time constant (stdev=1.93%)	First mode frequency (stdev=0.59%)
7.68 [sec.]	2.77 [Hz]	7.056 [sec.]	2.78 [Hz]

TAB. 2 Summary of laboratory test results on boom vibration damping

We can see that some damping effect is measured with high confidence of data accuracy although the amount of damping itself is small. The damping is more evident in the station#2 sensing than in the tip accelerometer (local effect is grater than global effect).

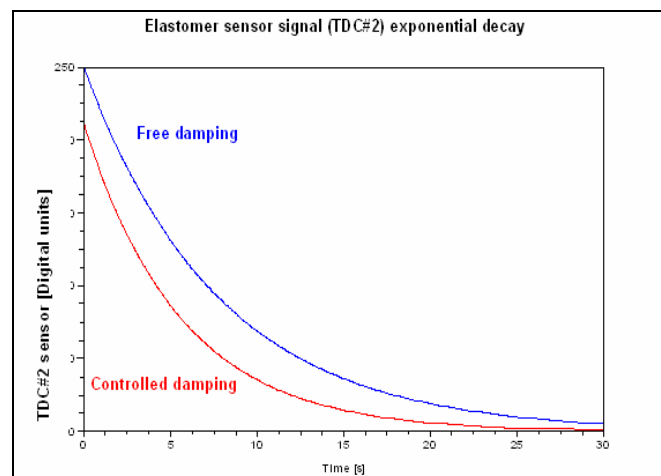


FIG. 25 Exponential decay of vibration seen from station#2 sensing

These experimental results were obtained after a few trials with different types of controls. We tried with a

Proportional Integrative Derivative (PID) control first but we did not achieve good results so, after numerical simulations, we switched to a derivative control with a threshold-ed non linear block. A block diagram of the implemented control is shown below

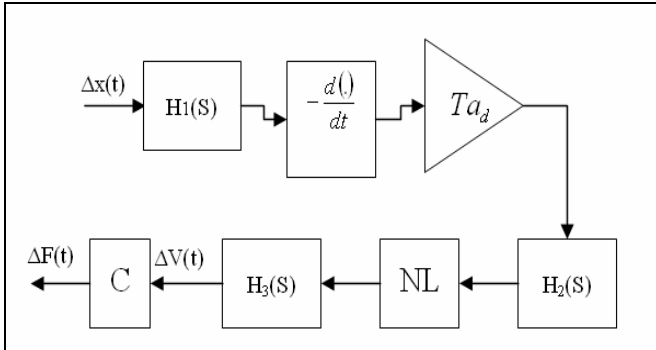


FIG. 26 Block diagram of the vibration damping control

$d(t)/dt$ → is the derivative operator

T_a → is an amplification factor

$\Delta x(t)$ → is the elongation variation of the EAP sensor

$\Delta V(t)$ → is the voltage variation of the EAP actuator

$\Delta F(t)$ → is the variation of the output equivalent force

H_1, H_2, H_3 → are linear filters

NL → is a non-linear block whose characteristic is shown below

C → is the block that describes the elastic force variation as a function of the applied

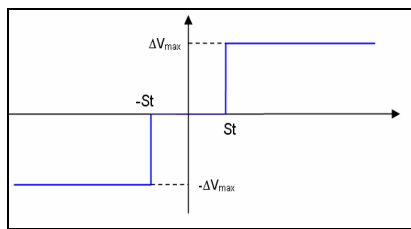


FIG. 27 Characteristic curve of the Non-Linear block

This kind of control appears to be more effective in damping the vibrations because the action of the elastomers is held at the maximum strength as long as the vibration itself is present and then set to null when the vibration falls below a threshold. The threshold also helps preventing unwanted oscillations due to the noise inherent to the high voltage modules and the noise generated by the derivative block.

The small amount of vibration damping achieved is due to the high stiffness of the boom compared with the actuation performances of the DEA-SCE configurations in terms of maximum force and stroke. The manufacturing process of the boom is rather complex and it was difficult to control the thickness of the carbon fibre which in the end resulted to be too stiff. Simulations carried out after the experimental tests have shown that a less stiff boom would have been

damped more effectively.

4.2. Bubble actuator

A single bubble actuator has been tested in a closed loop position control where the controlled parameter was the height of the bubble apex. Bubble was made to follow an height profile through a reference signal and also a disturb was introduced in the form of a small weight added on top of the bubble apex (see FIG. 28).

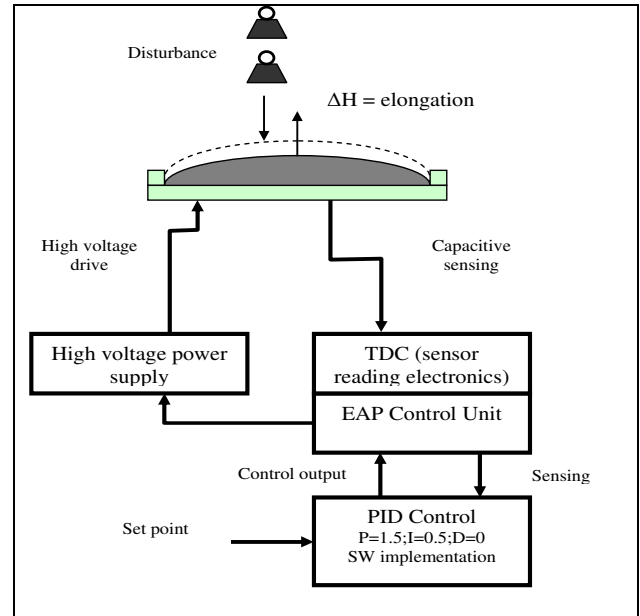


FIG. 28 Setup for the position control of a bubble actuator

The sensing signal for the control is represented by the integrated capacitive sensor whose characteristic curve is shown in FIG. 9. The control was of the Proportional –Integrative type and it was run in software under the LabVIEW© environment in a PC connected to the Electronic Control Unit. The graphs of FIG. 29 and FIG. 30 show the response of the various signals of the controlled system.

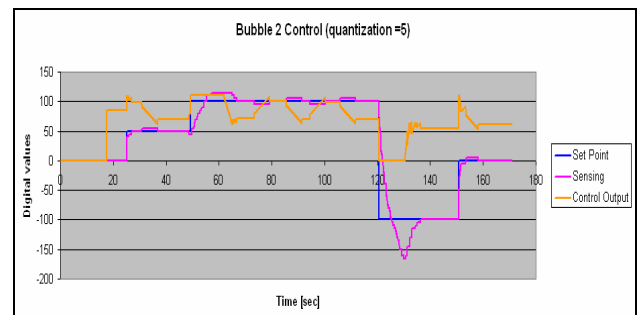


FIG. 29 Signals from controlled bubble actuator system: bubble follows set-point

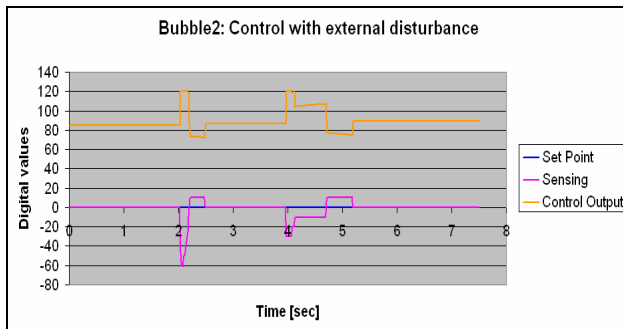


FIG. 30 Signals from controlled bubble actuator system: bubble responds to an external disturbance

5. CONCLUSIONS

The EAP project has gathered together important expertises from European academic and industrial partners in the fields of smart polymeric materials, smart space structures, space electronic systems and controls, and advanced simulation and modelling [8] [9]

Novel EAP configurations of integrated sensor-actuators have been devised, designed and manufactured with the aim of assessing their applicability to the monitoring and control of space structures[10]. The maturity of such class of devices has much improved and a number of problems have been identified and re-solved during the course of the project.

A broad range of aspects has been covered: material technology, structural integration electronic systems for actuating and sensing of EAP configurations. A great deal of work has also been done in the modelling and simulation of the configurations and the structures where they have been integrated for the manufacturing of the demonstrative breadboards.

In the scope the study the EAP technology has significantly matured and simple processes of mechanically interfacing EAP actuator/sensors have been found. The usability of EAP actuators on inflatable booms however is dependent on further progress on the inflatable materials (better dimensional accuracy, dry, semi cured CFRP half products) and on a progress on the actuators themselves (overload protection, higher forces and/or higher strokes). With higher forces and strokes also the damping capabilities will be improved as damping is related to the product of force and stroke. Pointing devices or shape control are other potential usages of EAP in space where bubble actuators show a high potential of application.

6. REFERENCES

1. *Sommer-Larsen, P.*, Polymer actuators - how do they work. In: Actuator 2004 - Conference proceedings. International conference on new actuators, Bremen (DE), 14-16 Jun 2004. Borgmann, H. (ed.), (Hanseatische Veranstaltungs-GmbH, Bremen, 2004) p. 681-685
2. *Benslimane, P.; Gravesen, P.; Sommer-Larsen, P.*, Dielectric elastomer actuators with smart metallic compliant electrodes. In:

- Conference proceedings. Actuator 2002 - 8. International conference on new actuators, Bremen (DE), 10-12 Jun 2002. Borgmann, H. (ed.), (Messe Bremen GmbH, Bremen, 2002) p. 383-387
3. *Sommer-Larsen, P.; Larsen, A.L.*, Materials for dielectric elastomer actuators. In: Electroactive polymer actuators and devices (EAPAD). Smart structures and materials 2004, San Diego (US), 14-18 Mar 2004. Bar-Cohen, Y. (ed.), (The International Society for Optical Engineering, Bellingham, WA, 2004) (SPIE Proceedings Series, 5385) p. 68-77
4. *Kofod G., Sommer-Larsen P.*, "Silicone dielectric elastomer actuators: Finite-elasticity model of actuation", SENSORS AND ACTUATORS A-PHYSICAL 122 (2): 273-283, 2005
5. *F. Carpi, G. Fantoni, P. Guerrini, D. De Rossi*, "Buckling dielectric elastomer actuators and their use as motors for the eyeballs of an android face", In Smart Structures and Materials 2006: Electroactive Polymer Actuators and Devices, Y. Bar-Cohen Editor, Proceedings of SPIE, Vol. 6168, pp. 61681A-1 - 61681A-6.
6. *F. Carpi, G. Fantoni, D. De Rossi*, "Bubble-like dielectric elastomer actuator with integrated sensor: device and applications", Proc. of Actuator 2006, Bremen, 14-16 Giugno 2006, H. Borgmann Editor, pp. 872-875].
7. *Gaudenzi P., Bathe K. J.* An iterative finite element procedure for the analysis of piezoelectric continua. Journal of Intelligent Material Systems and Structures, Vol. 6, 1995, 266-273.
8. *F. Carpi, P. Sommer-Larsen, D. De Rossi, P. Gaudenzi, L. Lampani, F. Campanile, E. Pfeiffer, G. Neri, S. Baldacci.* Electroactive polymers: new materials for spacecraft structures" European Conference on Spacecraft Structures, Materials & Mechanical Testing, 2005- ESA-ESTEC, Noordwijk, Holland
9. *F. Thurecht, E. Pfeiffer, S. Baldacci* Application of Electro Active Polymers to Very Large Space Structures" Adaptronic Congress 2006, 03-04 May, Göttingen, Germany
10. *C. Sickinger, L. Herbeck, T. Ströhlein, J. Torrez-Torres* Strukturmechanik Entfaltbarer Cfrp Booms: Analyse, Herstellung, Verifikation Und Anwendung Adaptiver Konzepte. Institut für Strukturmechanik, Deutsches Zentrum für Luft- und Raumfahrt e. V., Lilienthalplatz 7, D-38108 Braunschweig Deutscher Luft- und Raumfahrtkongress 2004, Deutsche Gesellschaft für Luft- und Raumfahrt, Dresden, Deutschland, 20.-23. Sep 2004